Experimental and Analytical Study of Scrap Tire Rubber Pad for Seismic Isolation

Huma Kanta Mishra, Akira Igarashi

Abstract—A seismic isolation pad produced by utilizing the scrap tire rubber which contains interleaved steel reinforcing cords has been proposed. The steel cords are expected to function similar to the steel plates used in conventional laminated rubber bearings. The scrap tire rubber pad (STRP) isolator is intended to be used in low rise residential buildings of highly seismic areas of the developing countries. Experimental investigation was conducted on unbonded STRP isolators, and test results provided useful information including stiffness, damping values and an eventual instability of the isolation unit. Finite element analysis (FE analysis) of STRP isolator was carried out on properly bonded samples. These types of isolators provide positive incremental force resisting capacity up to shear strain level of 155%. This paper briefly discusses the force deformation behavior of bonded STRP isolators including stability of the isolation unit.

Keywords—base isolation, buckling load, finite element analysis, STRP isolators.

I. INTRODUCTION

IT is growing concern for the designer to reduce the seismic demand instead of increasing the earthquake resistant capacity of the structure. This can be achieved by providing certain degree of flexibility in the structure by installing certain devices having low horizontal stiffness which is also known as the base isolation. The application of this technology all over the world is limited to the important and valuable structures due to its weight and incurred cost [1],[2]. Experience of the past earthquakes in developing countries suggests that the seismic performance of the structure could be significantly improved by the introduction of a simple seismic isolation system either at the construction or during the retrofitting stage. This would result in fewer building failure and decreased loss of lives during the past earthquake events [3].

A new type of seismic isolation system has been introduced using the scrap tire rubber as easily available material at low or negligible cost [4]. In literature, it can be found that the research on scrap tire pad has been initiated by Turer et al. [4]. In the previous study, the researchers produced the specimen samples and tested in vertical compression and in horizontal shear. The experimental test was conducted only stacking the samples one on top of another without using the adhesive. The car tire usually contents synthetic fiber as reinforcing cords.

Due to this reason, Turer et al. have mentioned that the scrap tire pad sample begins failure in compression at about 8.5MPa axial stress.

Huma Kanta Mishra is Ph.D. Candidate in Department of Urban Management, Kyoto University, Kyoto 615-8540, Japan (phone: 81753833246, e-mail: h.mishra@kt3.ecs.kyoto-u.ac.jp)

Akira Igarashi is Associate Professor in Department of Civil and Earth Resources Engineering, Kyoto University, Kyoto 615-8540, Japan (phone: 81753833245 fax: 81753833243 e-mail: igarashi.akira.7m@kyoto-u.ac.jp)

This result appears to show that the examined STRP isolators were insufficient for the practical use of scrap tire rubber pad in building isolation. In this paper, the results of experimental tests conducted on unbonded square STRP isolators and FE analysis conducted on bonded square STRP isolators are presented to investigate the factor to improve the performance of STRP isolators. The hyperelastic material constants used in FE analysis were derived by conducting uniaxial tension test of dumbbell shape rubber samples. The experimental test results were used to compute the mechanical properties of the STRP-6 isolator including stiffness and damping values. Based on the results of experimental test, the initial axial pressure was estimated by conducting the critical buckling load and stability analysis. Furthermore, stiffness of the isolators was computed using the established relationship and compared with the result of FE analysis. The results of FE analysis also provide the information about stress state within the STRP isolator.

II. STRP ISOLATORS

Only the rubber from the tread part of the scrap tire was used to prepare the specimen samples. The experimental test was conducted on the STRP samples just stacked one on top of another without applying the adhesive. The unbonded application allows rollover deformation. This rollover deformation decreases the effective horizontal stiffness of the isolator during the increase in lateral displacement which further increases the efficiency of the isolation system provided that stability is achieved [5]. The numerical investigation through finite element analysis was carried out to analyze the bonded STRP samples. These bonded samples would be produced by stacking one on top of another with the application of adhesive. The scrap tire rubber pad having physical dimensions of 100×100×72 mm (STRP-6) and 100×100×48 mm (STRP-4) were produced as shown in Figs. 1 (a) and (b). Each sheet of STRP layers consists of five layers of steel reinforcing cords interleaved in the rubber body. The rubber has shear modulus of 0.89MPa and hardness of 60 Durometer [6], [7]. The material and geometrical properties are presented in Table I.

TABLE I
MATERIAL AND GEOMETRICAL PROPERTIES [6], [7]

Material properties
Shear modulus of the tire rubber G = 0.89 MPa
Young's modulus of the steel cords E = 200 GPa
Poisson's ratio of the steel reinforcing cords υ = 0.3
Geometrical properties (mm)
Size of the STRP = 100×100
Thickness of a single STRP layer = 12
Total thickness of STRP-6 = 72, t_r = 60
Total thickness of STRP-4 = 48, t_r = 40

World Academy of Science, Engineering and Technology
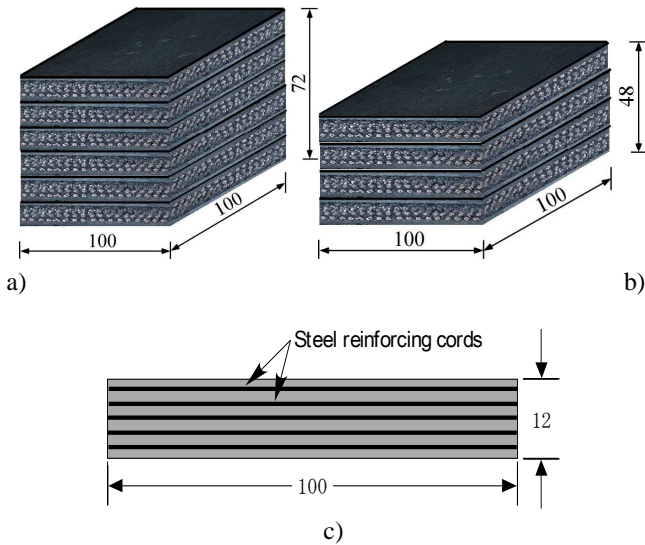International Journal of Civil and Environmental Engineering
Vol:6, No:2, 2012

Fig. 1 a) Six layers(STRP-6) isolatorb)four layers (STRP-4)c) Single layer STRP isolator

III. EXPERIMENTAL SETUP AND TEST

Figure 3 shows schematic view of the test set up which was designed to perform both the vertical and horizontal loading test. The STRP-6 isolator was placed between the upper and lower steel plate surfaces of the load test setup. The vertical load was applied to the specimen by the vertical hydraulic actuator in displacement control. The vertical hydraulic actuator had a maximum loading capacity of ±400kN and maximum displacement capacity of ±50mm in the vertical direction. The horizontal load was applied in displacement control by a horizontal hydraulic actuator with a load capacity of ±400kN and a maximum displacement of ±125mm.
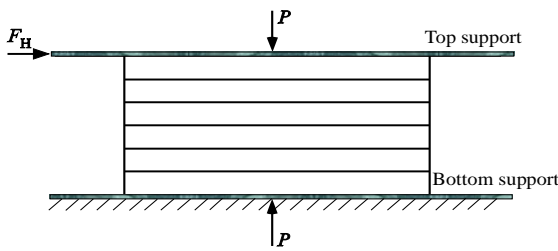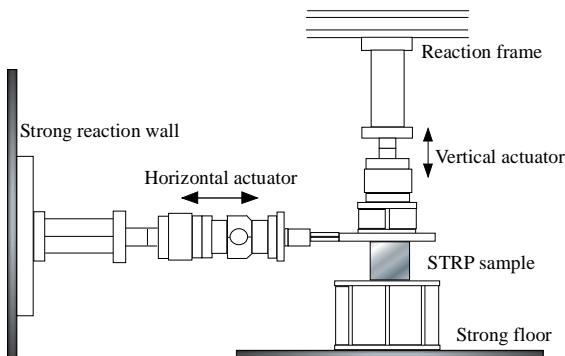

Fig. 2 Loading setup for STRP isolator

Fig. 3 Schematic view of test set up

A. Compression Test

The compression modulus and the maximum vertical deflection of the bearings were evaluated through vertical compression testing. The STRP-6 specimen samples were tested under vertical displacement control. The specimen was monotonically loaded to the equivalent vertical force of 91.9KN and is equivalent to 9.19MPa vertical pressure on STRP-6 sample. In the final stage of the vertical testing, the specimen was monotonically unloaded. Additionally, under a constant vertical compressive pressure the isolators were subjected to horizontal static shear loading.The test results are shown in Fig. 4.
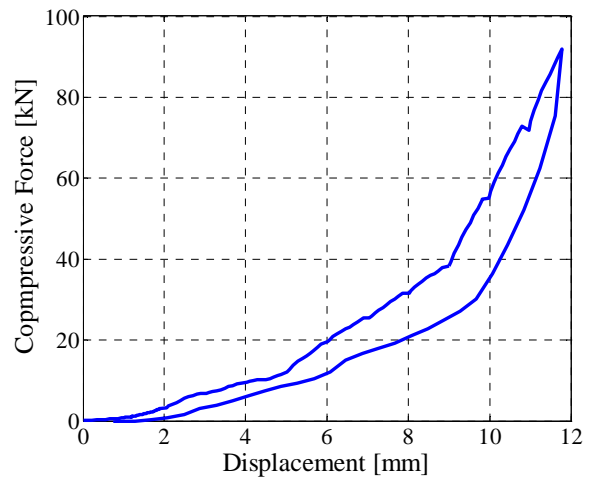

Fig. 4 Vertical load-deflection relationships of STRP-6

B. Shear Test

The purpose of the monotonic shear tests was to evaluate the maximum shear deformation capacity and possible residual slip of the unbonded STRP-6 isolator at constant vertical load. The specimen sample was tested at six maximum shear displacement amplitudes of 12mm, 24mm, 36mm, 48mm, 60mm, and 62mm. These displacement amplitude cycles were applied at a constant vertical pressure of 5MPa. During the complete experimental testing, no residual slip was observed. Results of monotonic shear test are shown in Figs. 5 and 6.
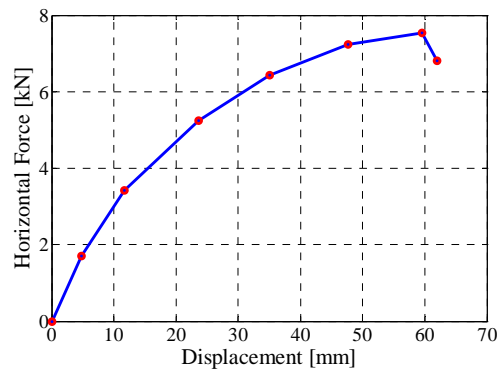

Fig. 5 Force-displacementrelationship of STRP-6; experimental results

World Academy of Science, Engineering and Technology
International Journal of Civil and Environmental Engineering
Vol:6, No:2, 2012

Fig. 6 Deformed STRP-6 at 103% lateral deformation

IV. STABILITY AND BUCKLING LOAD

During the strong earthquake shaking, seismic isolators have to sustain large shear deformation and have to maintain the stability. This requires the determination of critical axial load on the isolator at its extreme deformation condition. The main purpose of the study is to investigate whether the STRP isolator needs additional improvement in order to increase the axial load carrying capacity or it can withstand the axial load designed for low rise residential building. The thickness of the single STRP is 12 mm on an average. By using these STRP layers, sufficiently large size bearing production is possible. Increasing the number of layers shall increase the isolator thickness which helps in lengthening the time period of the structure [8]. However, the shear flexibility of the short columns can lead to relatively low buckling loads which may be further reduced for greater shear deformation. The assessment of stability of seismic isolation bearing is essential in order to ensure that the single bearing or whole isolation system along with the building structure is stable during the large earthquake events which produce large lateral displacement. In order to evaluate the stability of the isolation system, the extreme buckling load on isolator during extreme lateral displacement shall be evaluated. Generally, Haringx's theory is used to evaluate the critical buckling load for a single isolation unit [9]. The current approach to calculate the critical load on an isolator is to use the Haringx's theory as givenby (1) which is further modified for increased shear deformation [10].

$$P_{cro} = \frac{(GA_s)_{eff}}{2}\left[\sqrt{1 + 4\frac{P_E}{(GA_s)_{eff}}} - 1\right] \tag{1}$$

$$P_E = \frac{\pi^2 (EI)_{eff}}{h^2} \tag{2}$$

where PE is the Euler's load, $(GA_S)_{eff}$ is the effective shear rigidity, $(EI)_{eff}$ is the effective flexural rigidity, E is the bending modulus, G is the shear modulus of rubber, I is the moment of inertia of the bearing about the axis of bending and h is the effective height of the rubber bearing including rubber and steel and the values depends on the boundary condition of the isolation bearing. If t_r is the total thickness of rubber, then shear rigidity and flexural rigidity can be expressed as

$$(GA_s)_{eff} = GA\left(\frac{h}{t_r}\right) \tag{3}$$

$$(EI)_{eff} = E_r I\left(\frac{h}{t_r}\right) \tag{4}$$

where E_r is the bending modulus given by (5)[11].

$$E_r = E_0(1 + 0.742S^2) \tag{5}$$

where E_0 is the elastic bending modulus of rubber, approximately equal to four times the shear modulus, S is shape factor shown in (6) and (7).

The shape factor of the bearing is given by

$$S = \frac{A_u}{A_c} \tag{6}$$

where A_u is the loaded area and A_c is the force free area. For square bearing with side b and single layer thickness t, the shape factor S is given by

$$S = \frac{b}{4t} \tag{7}$$

The compression modulus is given by

$$E_c = nGS^2 \tag{8}$$

where n is a constant that depends on the shape of the bearing and equal to 6.73 for a square bearing.

In order to account for the large displacement during large earthquakes, some approximation formula have been devised in the above formulations [9]

$$P_c = P_{cro}\frac{A_r}{A} \tag{9}$$

where P_c is the critical load in the current configuration, P_{cro} is the critical load on the undeformed configuration, A is the base area of the bearing and A_r is the projected base area of the bearing in its current configuration as shown in Fig.7.[12]

World Academy of Science, Engineering and Technology
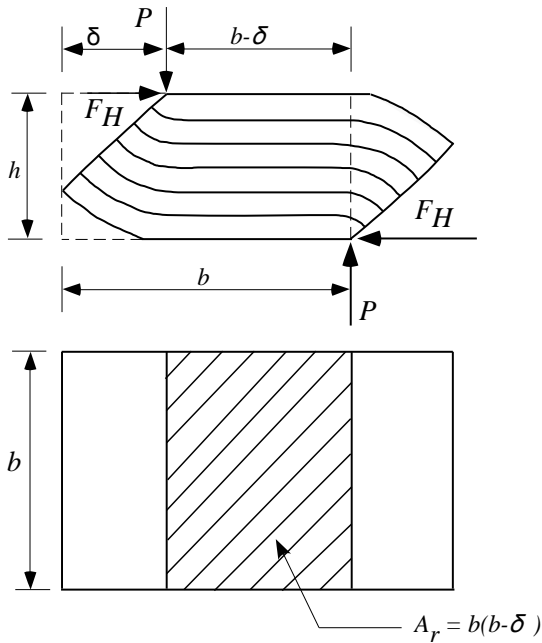International Journal of Civil and Environmental Engineering
Vol:6, No:2, 2012

Fig. 7 Stability and overlap area

The calculated critical load using the dimensions and material constants of STRP-6 samples is shown in Fig. 8. The critical buckling load can be converted to the nominal axial stress, i.e. the vertical axial pressure at zero lateral deformation, as shown in Fig. 9.

From Figs.5 and 9, the estimated critical nominal axial stress has a close agreement with the experimental result. The estimated initial stress to achieve 60mm lateral displacement is about 5.7MPa and the axial stress applied during the test was 5MPa. The force-deflection plots for all tests should have a positive incremental force-resisting capacity to be used as base isolation device [13]. The force displacement relationship obtained by experimental test provide positives incremental force resisting capacity up to 60mm lateral displacement and it drops to negative scant stiffness.
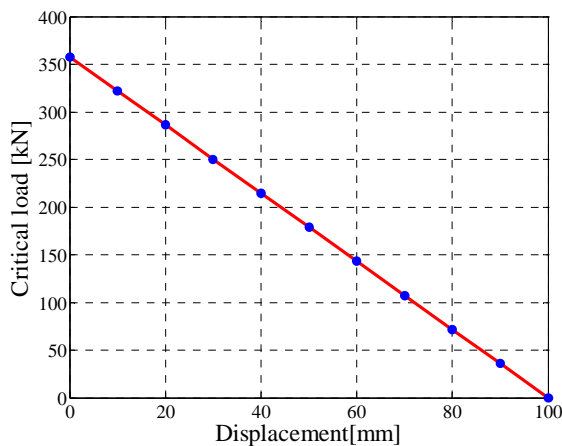
This result indicates that the initial axial stress estimated using the buckling load analysis can be considered as reference values even the samples were prepared without applying the adhesive. The shape factor of the tested samples was 10.4 and aspect ratio 1.4 which results in lower lateral displacement capacity. Due to this reason, the STRP-4 samples are prepared bystacking theSTRP layers one on top of another with the application of adhesive in between the layers which has aspect ratio greater than two.
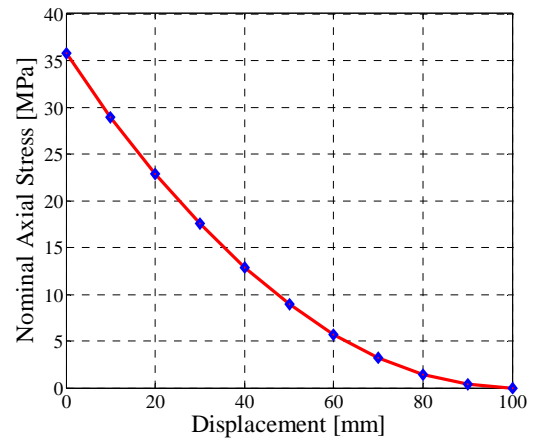

Fig. 9 Nominal axial stress calculated from the critical buckling load for STRP-6

In this regard, the STRP-4 samples may sustain larger level of lateral deformation compare to STRP-6. Similar methodology was adopted to estimate the initial axial stress on STRP-4 and is shown in Fig.10 and 11. The estimated initial axial pressures of 8.6MPa wereutilizedin FE analysis of STRP-4 isolator.
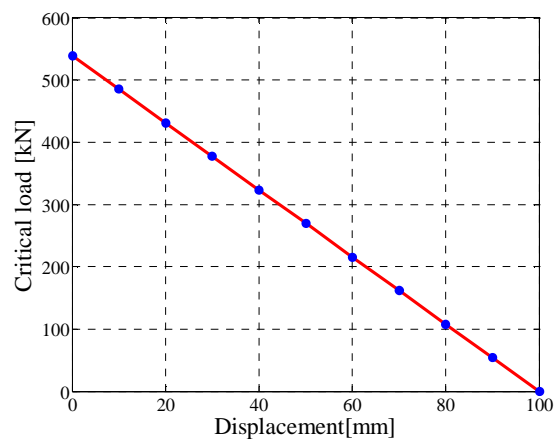

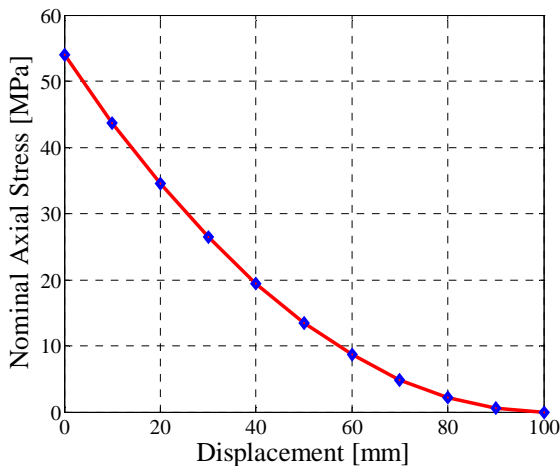Fig. 10 Relationship between the theoretical buckling load and lateral displacement for STRP-4

Fig. 8 Relationship between the theoreticalcritical buckling load and lateral displacement for STRP-6

World Academy of Science, Engineering and Technology
International Journal of Civil and Environmental Engineering
Vol:6, No:2, 2012

Fig. 11 Nominal axial stress calculated from the critical buckling load
for STRP-4

V. Finite Element Analysis

The STRP is composed of a rubber body with embedded steel reinforcing cords. Finite element analysis of strip STRP was conducted using general purpose finite element software [14]. The rubber part was modeled using quadrilateral elements. The reinforcing steel cords were modeled by rebar elements. The hyperelastic material model described by the strain energy density function expressed by (10) with the identified constants was utilized to model the rubber body.

$$W = C_{10}(I_1 - 3) + C_{01}(I_2 - 3) + C_{11}(I_1 - 3)(I_2 - 3) + C_{20}(I_1 - 3)^2 + C_{30}(I_1 - 3)^3 + \cdots \quad (10)$$

where I_1 and I_2 are the first and second invariants of the strain tensor, and C_{10}, C_{01}, C_{11} C_{20}, and C_{30} are the material constants known as the Mooney-Rivlin material constants which have the unit of stress.

The steel reinforcing cords in finite element model is treated as bars of linear elastic isotropic material[7] with material properties given in Table I. The orientation of the cords with respect to global x-axis is shown in Fig. 12.
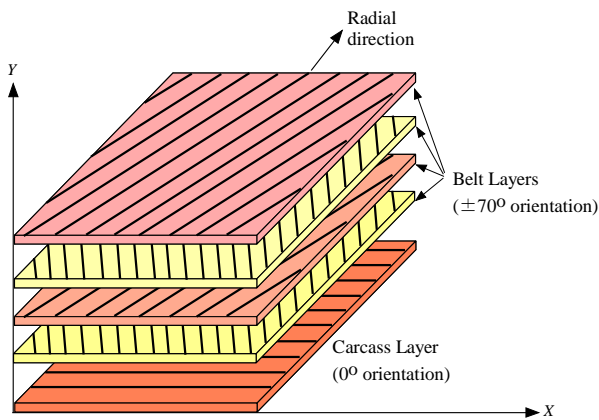

Fig. 12 Layout of steel reinforcing cords in a single layer STRP

The hyperelastic material constants used in the FEanalysis were derived by a uniaxial tension test of dumbbell shape rubber samples and are presented in Table II.

TABLE II
MOONEY-RIVLIN MATERIAL CONSTANTS

Rubbermaterial constants (MPa)	$C_{10} = 0.40000$
	$C_{01} = 1.22315$
	$C_{11} = 0.18759$

Two horizontal rigid bodies (lines) were defined at the top and bottom of the STRP isolator to represent the superstructure and substructure, respectively. In this model, the vertical and horizontal loads were applied on the top support; the top support was allowed to move in vertical and horizontal directions while the bottom support was considered as a fixed support. In this contact model, the contact between the supports and the STRP isolator was modeled by the Coulomb friction law with a coefficient of friction 0.8. The coefficient of friction was selected such that no slips occur between the contact support and the rubber. The STRP isolator is not bonded to the top and bottom support contact surfaces and its rollover deformation was allowed.

At the initial stage of the analysis, the target compressive pressure of 8.6 MPa was applied with different incremental steps. Then the horizontal load was applied with the constant compressive load until a target lateral displacement was achieved. Due to the rollover deformation, the effective horizontal stiffness decreases with increased lateral deformation. This results in elongation of the time period of the isolation system, as well as an eventual instability at the displacement level of 62mm, corresponding to 155% shear strain (based on the thickness of rubber). The results of FE analysis are presented in Figs. 13 through 16.
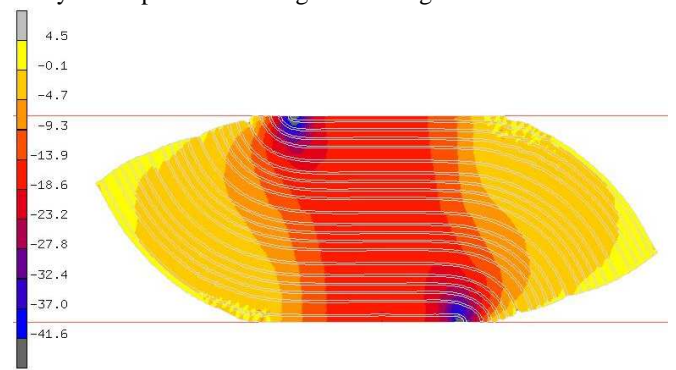

Fig. 13 Contour of normal stress S_{22} (MPa) in the rubber layers of the
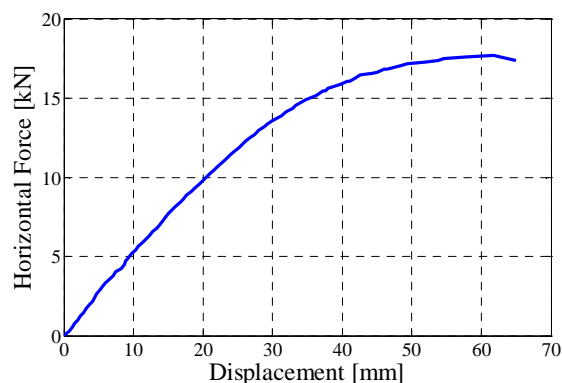STRP-4 isolator at 155% lateral displacement

World Academy of Science, Engineering and Technology
International Journal of Civil and Environmental Engineering
Vol:6, No:2, 2012

Fig. 14 Load-displacement relationship of the STRP-4

A. Finite Element Analysis Results and Discussion

The vertical stiffness of the STRP-4 was calculated by using the conventional established relationship $K_V = E_cA/t_r$. The vertical stiffness with the values given elsewhere in this article is 144145.7kN/m. Similarly, the horizontal stiffness of STRP-4 isolator using the conventional relationship $K_H = GA/t_r$, is 222.5kN/m. The horizontal effective stiffness of the STRP-4 isolator using the FE analysis result corresponding to 60mm lateral deformation is 293.95N/m. The ratio between vertical and horizontal stiffness is calculated as 490.4. This result indicates that the STRP-4 isolator can be used as base isolation device considering a specification explored in Eurocode 8 [15]. The lateral load displacement relationship for STRP-4 isolator is shown in Fig. 14. As seen in this figure, the STRP isolator behaves nonlinearly due to the rollover deformation. This type of deformation decreases the effective horizontal stiffness with increased lateral displacement. When stiffness is decreased, the period of isolation consequently increased which can be considered as increase in isolation efficiency. In the design of seismic isolators, the isolator should produce positive incremental force resisting capacity throughout the entire range of the lateral displacement [13]. This means that the STRP-4 isolator can be used as base isolation device to achieve the target lateral displacement up to 62mm (155% of the thickness of rubber). The stress state and shear strain distribution within the STRP-4 is shown in Figs. 13 and 15 respectively.
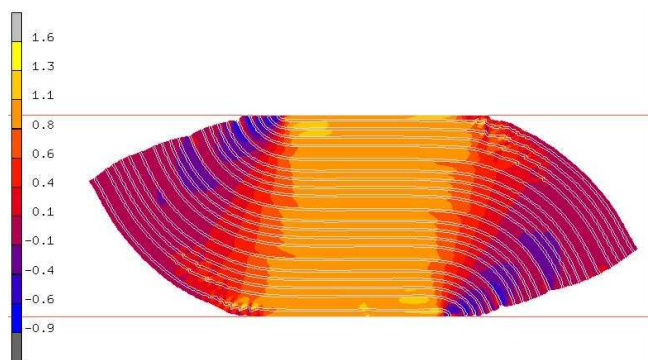

Fig. 15 Shear strain distribution within the STRP-4 isolator at 155% lateral displacement
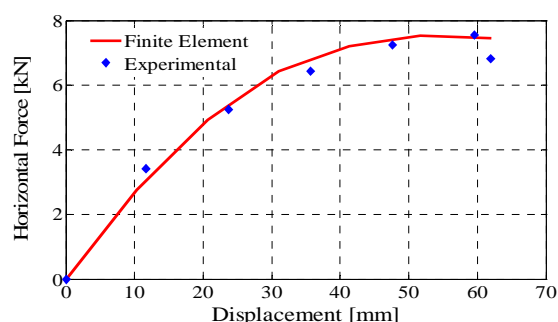

Fig. 16 Load-displacement relationship of the STRP-6; comparison between finite element analysis and experimental results

In order to validate the finite element model, force-displacement relationship obtained from FEanalysis was compared with experimental test result for STRP-6 isolator. As seen in Fig. 16, a reasonable agreement was found between the experimental results and the FEanalysis results. However, for lower level lateral displacement, the accuracy of the FEanalysis is noticed to be lower than the experimental results. The reason behind this may be the negligence of strain dependency of the steel reinforcing cords and rubber material [5] in FE analysis. The hyperelastic material constants derived by the uniaxial tension test results assumed to be the real representative of the tire rubber. The results of FE analysis were used to calculate the effective horizontal stiffness and stability analysis. Due to the rollover deformation, the effective horizontal stiffness decreases with increase in lateral displacement which further elongates the natural period of the structure. There is a close agreement between the critical buckling load and the FE analysis result. These STRP-4 isolators have positive incremental load resisting capacity up to shear strain level of 155%. The STRP-4 isolator is considered stable up to lateral displacement of 155% (based on the thickness of rubber). The ratio between the vertical and the horizontal stiffness is greater than 150 so that the isolator can be used as base isolation device [15]. Vertical axial pressure of 8.6MPa can be considered appropriate for low rise building structures.

VI. CONCLUSION

A new type of seismic isolation system using STRP (Scrap Tire Rubber Pad) has been introduced as a cost-effective material with a wide availability, intended to be used in low rise residential buildings of highly seismic areas of the developing countries. The compression tests and monotonic shear loading tests on unbonded 6-layer STRP isolator specimens were conducted, and the test result shows that the STRP isolators have horizontal load capacity up to the shear strain level of 100%. A good agreement between the result of stability analysis of the STRP isolators considering accounting for large horizontal displacements and the test results is obtained. Finite element analysis of a 4-layer bonded STRP isolator indicates that STRP isolators can show acceptable performance that can be used as a base isolation device for earthquake protection of low rise residential buildings. However, the results of FE analysis have to be verified by experimental testing which is planned in the future research.

REFERENCES

[1] James M. Kelly, Dimitrios Konstantinidis. Low-cost seismic isolators for housing in highly-seismic developing countries. 10th World Conference on Seismic Isolation, Energy Dissipation and Active Vibrations Control of Structures, Istanbul, Turkey, May 28-31, 2007

[2] James M. Kelly. Seismic isolation system for developing countries, Earthquake Spectra, 2002, Vol. 18, issue 3:385-406.

[3] Hamid Toopchi-Nezhad, Michael J. Tait, Robert G. Drysdale. Testing and modeling of square carbon fiber-reinforced elastomeric seismic isolators. Structural Control and Health Monitoring, 2008, 15: 876-900.

[4] Ahmet Turer and Bayezid Ozden. Seismic base isolation using low-cost Scrap Tire Pads (STP). Material and Structures, Vol. 41, 2008, 891-908.

[5] Hamid Toopchi-Nezhad, Michael J. Tait, Robert G. Drysdale. Bonded versus unbonded strip fiber reinforced elastomeric isolators: Finite element analysis. Composite Structures, 93(2011):850-859.

[6] Y.J. Arditzoglou, J. A. Yura and A. H. Haines. Test methods for elastomeric bearing on bridges. Research Report 1304-2, Texas Department of Transportation

[7] H. Holcher, M. Tewes, N. Botkin, M. Lohndorf, K. H. Hoffmann, E. Quandt. Modeling of pneumatic tires by a finite element model for the development of a tire friction remote sensor. Center of Advanced European studies and Research (Caesar), (2004), 40.

[8] Jong She Lee and Long Won Oh. Stability of rubber bearings for seismic isolation. Transactions of the 15th International Conference on Structural Mechanics in reactor technology, Seol, Korea, August 15-20, 1999.

[9] Gabriela Ferraro, Giuseppe Oliveto and Nicholas D. Oliveto. On the stability of elastomeric bearings. Department of Civil and Environmental Engineering, University of Catania, Italy.

[10] Ian Buckle, Sathish Nagarajaiah and Keith Ferrell. Stability of elastomeric isolation bearings: Experimental Study. Journal of Structural Engineering, vol. 128, No. 1, January 2002.

[11] R. Lo Frano and G. Forasassi. Evaluation of instability of Laminated Rubber Bearings under dynamic loading. Proceeding of ICAPP '10', San Diego, USA, 2010.

[12] Farzad Naeim, James M. Kelly. Design of seismic isolated structures from theory to practice. John Willey and sons, Inc. 1999, chapter 6.

[13] ASCE-7. Minimum design loads for building and other structures, ASCE/SEI 7-05. New York, American Society of Civil Engineers, 2005.

[14] MSC Software (2010), MSC Marc 2010 and MSC Marc Mentat 2010, Santa Ana, California

[15] Eurocode 8. Design of structures for earthquake resistance. 2004